Phase transition of sulfur during the compression by laser-induced nano-shock

Shuji Ye, Mitsuo Izumo, Masataka Sakai, and Mitsuo Koshi[†]

Department of Chemical System Engineering, School of Engineering, The University of Tokyo, 7-3-1 Hongo, Bunkyo-ku, Tokyo 113-8656, JAPAN
[†] Corresponding address: koshi@chemsys.t.u-tokyo.ac.jp

Abstract

A time-resolved Raman system was constructed to observe the shock response of sulfur powder under the laser-driven shock compression conditions. The local pressure was estimated on the basis of the Rankine-Hugoniot relation and the particle velocity measured by VISAR (Velocity Interferometer System for Any Reflector). Maximum pressure obtained by the present apparatus was estimated to be 0.75 GPa. It is found that the Raman intensities behind the shock wave decreased rapidly (within 50 ns), and the intensity did not recover after the shock compression. The melting of the crystal, or the formation of amorphous sulfur can explain these observations. The vibrational temperature corresponding to the line at 218 cm^{-1} was higher than the bulk temperature behind the shock wave.

Keywords: Laser shock, High pressure, Phase transition, Sulfur

1. Introduction

The study of sulfur, especially at high pressure, has been paid many attentions for a long time since sulfur is of relevance in geophysics, astrophysics, material sciences, and massively used in industry [1]. Sulfur can exist in more than thirty solid modifications, which consist of S_6, S_7, S_8, S_9, S_{10}, S_{12}, S_{18}, S_{20}, and polymeric chain molecules under different temperature and pressure [1].

Under normal temperature and pressure, orthorhombic sulfur is in most stable form known as α-S_8, a molecular crystal built by crown shaped S_8 rings in D_{2h}^{24} symmetry [1, 2]. The phase change under high pressure has been observed by many authors using Raman scattering and X-ray diffraction methods [3, 4]. The previous studies indicate that the pressure and photo-induced phase transitions depend on pressure, sample impurity, photon energy, and laser power [3, 4]. The phase sequence α-S_8 → a-S (amorphous) → p-S (high-pressure unknown phase) → S_6 (high pressure high temperature phase) was found up to 15 GPa [3, 4].

The phase change in sulfur is generally believed to be caused by the small energy gap between HOMO (highest occupied molecular orbital) and LUMO (lowest unoccupied molecular orbital), that is, a small band gap. At ambient pressure, the indirect band gap of α-S_8 was reported to be 2.6 - 2.9 eV based on the optical absorption spectra [5, 6]. The absorption edge depends sensitively on impurities. With pressure increasing, the band gap becomes smaller [7, 8]. The band gap becomes 0 above 50 GPa, and metallization of sulfur could be observed [7].

Photo-excitation from HOMO to LUMO causes a bond breaking of S_8 ring and as a result, S_8 chain is produced [3, 4, 8-10]. The sulfur changes into amorphous phase because of this bond breaking. With the formation of amorphous phase, Raman peaks become weak in intensity and broad [3, 4, 11]. These high hydrostatic pressure studies indicated that the mechanism of phase change in sulfur is the HOMO-LUMO excitation mechanism.

Although many studies on the phase transition of sulfur under high hydrostatic pressures have been performed, physical or chemical changes of sulfur have not been studied under the dynamic high pressure. Shock waves in condensed matter provide a way of very rapidly attaining extreme conditions of high pressure, high density, and high temperature [12, 13].

Shock compression of crystals will cause large-amplitude mechanical deformations. Little is known on the shock-induced chemical reaction in molecular solids [14]. In this paper, we report the changes in sulfur crystal caused by the laser-driven shock compression.
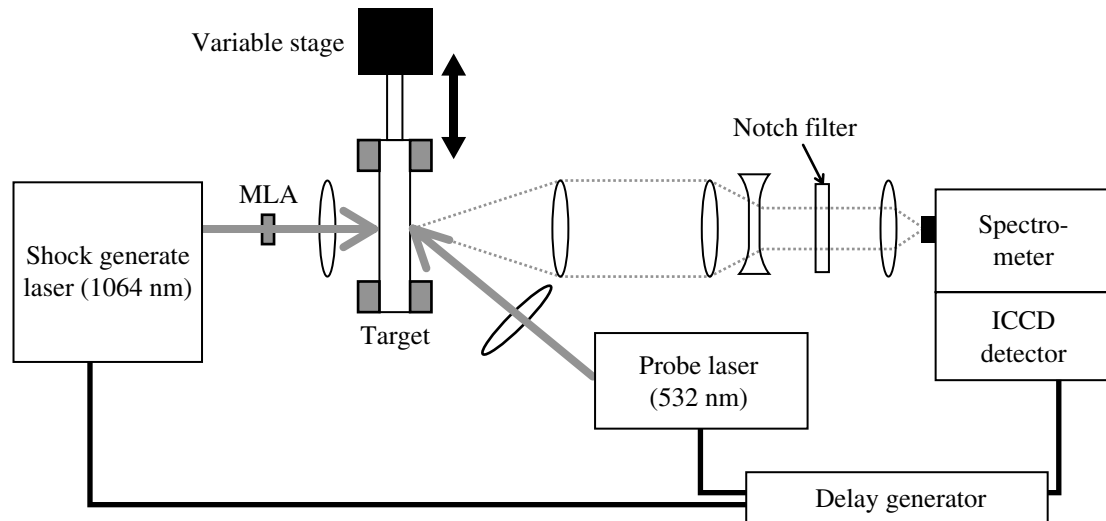
Fig. 1 A schematic of experimental apparatus for the time resolved Raman measurement after the laser-driven shock compression. (MLA : Multi lens array)

2. Experimental

A schematic of the experimental apparatus is shown in Fig. 1. The fundamental light of Nd:YAG laser (1064 nm, 500 mJ pulse^{-1}, FWHM = 10 ns) was used for shock generation and the second-harmonic light (532 nm, 1 mJ pulse^{-1}, FWHM = 10 ns) of the other Nd:YAG laser was used for exciting Raman scattering. The delay between the probe (532 nm) and pump (1064 nm) laser was controlled by a digital delay generator (DG 535). The fundamental light for the shock generation was focused on the target through a multi lens array coupled with a normal lens (f = 250 mm) to produce the flat shock waves. Raman scattering was collected with a lens, spectrally resolved by a monochromator (McPHERSON, MODEL 2035) with a 1200 lines mm^{-1} grating, and detected by a 576 × 384 pixel intensified CCD camera (Princeton instruments, ICCD-576 G(R&B) with ST-138 controller). The resolution of monochromator is 5.4 cm^{-1}. Holographic notch filter (Kaiser, SuperNotch-Plus™ 6.0, FWHM = 350 cm^{-1}) was used to reject Rayleigh scattering.

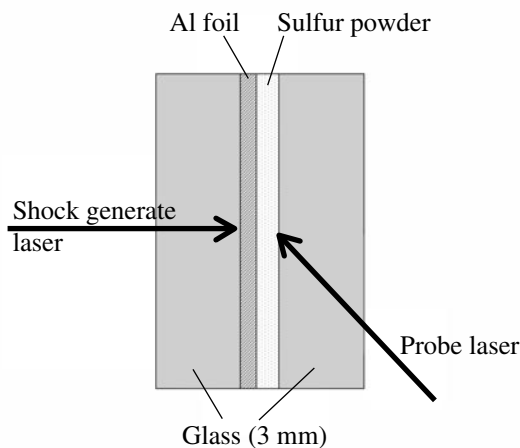The target is composed of a back-up glass (40 mm ×

Fig. 2   Structure of target sample.

40 mm × 3.0 mm), an aluminum foil, sample, and a cover glass (40 mm × 40 mm × 3.0 mm), as shown in Fig. 2. Aluminum foil was adhered to the back-up glass by epoxy resin. Laser-induced plasma was generated between the sample and the back-up glass and drove a shock wave through the aluminum foil into the sample.

The pressure P in the sample was estimated on the basis of the conservation equation of momentum.

$$P = P_0 + \rho_0 U_s U_p \qquad (1)$$

Here, P_0 is an initial pressure, ρ_0 is a density (2.07 g cm^{-3}), U_s is a shock velocity and U_p is a particle velocity. The shock velocity U_s is estimated by the Hugoniot equation, $U_s = A + B\ U_P$, where A, B are constants. The Hugoniot equation of sulfur is very complex. It depends on the factors such as the sample impurity and sample density. The Hugoniot equation given in LASL Shock Hugoniot Data (ρ_0 = 2.02 g cm^{-3}) [15] is given by;

$$U_s = 3.633\ (\pm\ 0.013) + 0.606\ (\pm\ 0.010)\ U_p,$$
$$0.897\ \text{km s}^{-1} \leq U_p\ 1.470\ \text{km s}^{-1}.$$

$$U_s = 2.8\ (\pm\ 0.3) + 1.18\ (\pm\ 0.15)\ U_p,$$
$$1.431\ \text{km s}^{-1} \leq U_p \leq 2.046\ \text{km s}^{-1}$$

Gogulya et al. [16] also reported another U_s - U_p relation.

$$U_s = 2.26 + 1.71\ U_p - 0.039 U_p^2,$$
$$0.5\ \text{km s}^{-1} \leq U_p \leq 2.91\ \text{km s}^{-1},\ \rho_0 = 2.07\ \text{g cm}^{-3}.$$
$$(2)$$

This equation is used to calculate U_s from the measured U_p, since the valid range of U_p is closer than the LASL data to the present experimental conditions.

The particle velocity profile was measured with a VISAR (Velocity Interferometer System for Any Reflector, ATA Associates 605-FCV). By using 4 etalons with this VISAR
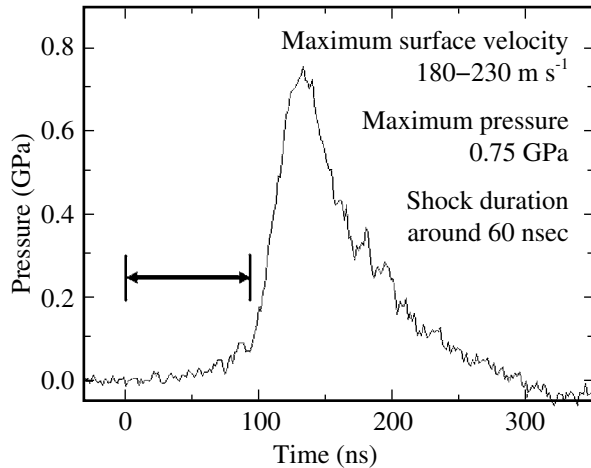
Fig. 3   An example of the pressure profile derived form U_p measured by the VISAR. (30 μm Al foil, 55 μm sulfur layer).
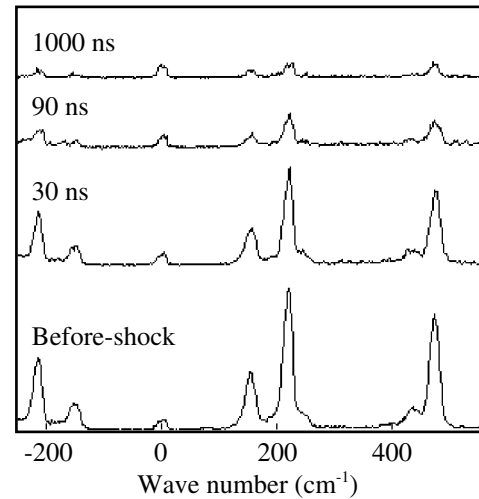

Fig. 4   Examples of the time-resolved Raman spectra observed at different time delay between shock and probe laser. Each spectrum was averaged over 10 laser shots. (30 μm Al foil, 55 μm sulfur layer)
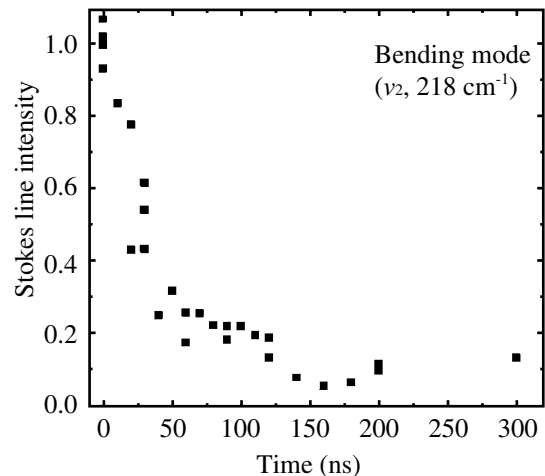
system, one fringe of the interferogram corresponds to 503 m s^{-1}. Time profiles of particle velocity (and hence pressure) strongly depend on the thickness of aluminum and sample. An example of a pressure profile is shown in Fig. 3 that is average over 10 laser shots (50 μm Al foil, and 55 μm sample layer). Maximum particle velocity in the present experiments was 205 ± 20 m s^{-1} and maximum pressure was estimated to be 0.88 ± 0.17 GPa. Typical shock duration was about 60 ns. Although particle velocities in these experiments are lower that the valid range for the equation (2), the contribution of U_p-dependent parts to U_s in the equation (2) is small at the values of U_p in the present experiments.

In Fig. 3, there is a time delay of about 100 ns before the onset of the pressure rise. The origin of this time delay is not clear. The time t=0 in Fig. 3 is defined by the time of the fire of the shock generating YAG laser which is measured by a pin photo-diode. In order to clarify the origin of this delay, U_p was measured by changing the thickness of the Al foil without the sample sulfur. The delay time was linearly dependent on the thickness of the Al foil, but the extrapolation to zero-thickness still gave the delay time of 33 ns. This 33 ns delay could be attributed to the delay in our VISAR system. In addition, the time for the shock propagation through an Al foil (8 ns) has to be added to the delay time. However, the observed delay time (100 ns) is still longer the sum of these delays time (33 + 8 = 41 ns). Residual delay may be attributed to the time for the shock propagation in the sulfur sample, because our VISAR may probe the back surface of the sample. In addition, the time for the relaxation processes of the internal energy in sample can also contribute to this delay. Further work is needed to clarify the origin of this delay time in U_p, (and hence in pressure).

Sample of sulfur was bought from Aldrich chemical Co. with a purity of 99.998 + % (ρ_0 = 2.07 g cm^{-3}) and was used without further purification.

Fig. 5   A time profile of the Raman intensity at 218 cm^{-1}.

3. Results and discussion

The Raman spectral change with the delay time is shown in Fig. 4. Raman shift and intensity were calculated by fitting the spectral line profile to a Gaussian function. It was found that the Raman intensities behind the shock wave decreased very rapidly, and did not recover even after the shock compression. This phenomenon of intensity decrease was common in all experiments. Figure 5 shows a time profile of Raman intensity at 218 cm^{-1}. As shown in the figure, the decay is completed within 50 ns. Similar decay rates were also observed in the mode at 475 cm^{-1}, as shown in Fig. 4. In these experiments, the color of the sample has changed into pale yellow in the shocked region. Therefore physical properties of sulfur are changed by the shock compression.

Raman spectral shifts were observed by several researches in the static compression experiments of sulfur [11), 17), 18)]. According to these static pressure experiments, the fre-

quency shift below 1 GPa is less than 4 cm⁻¹. This shift is narrower than the wavelength resolution of the present detection system (FWHM of 5.4 cm⁻¹). NO obvious frequency shift was confirmed in the pressure range of the present experiments.

There are several possibilities to explain the observed change in sulfur. One possibility is the transition into the amorphous phase. With the formation of amorphous sulfur, Raman intensities are known to become very weak [3), 4), 11)]. Transition from the α-S_8 phase to amorphous could be induced by the photo-excitation [3), 4)], and the 532 nm probe laser light can be responsible for the photo-excitation. The band gap of the α-S_8 sulfur is in the range of 2.7-2.9 eV at ambient pressures. This band gap becomes smaller as pressure increases [3)], and the band gap possibly becomes small enough to absorb 532 nm photon (2.33 eV) because of the shock compression. According to the static compression experiments by Eckert et al. [3)], the band gap of sulfur becomes comparable with the photon energy of 532 nm lights at the pressure of 3-4 GPa. This pressure range is much higher than the present dynamic pressure (0.75 GPa). Therefore, this photo-excitation mechanism is less likely for the present shock compression experiment. Further studies are required to conclude the validity of this mechanism.

It is well known that the phase transition from the α-S_8 phase into a monocline phase (β-S_8) occurs at the static pressure of 5.3 GPa without the photo-excitation [3)]. In this case, the S_8 ring structure holds in the monocline phase, and therefore, it is expected that Raman intensity does not change significantly by this phase transition. And the transition pressure is too high compared with the present peak pressure. This high-pressure phase transition may not be responsible for the fast decay of the Raman intensity.

Phase transition from the solid α-S_8 to liquid is another possibility. Solid to liquid transition is known to occur at T=386 K and P=1 atm. In the present dynamic compression experiments, the temperature of the sample is also increasing behind the shock wave. This temperature increase can cause the melt of the sample. Further heating
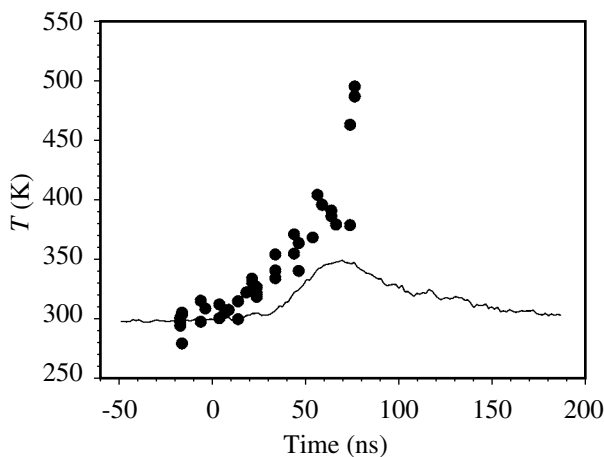
of the liquid sample will cause the breaking of S_8 ring and will start the polymerization at T=432 K [19), 20)]. These bond breaking and polymerization also induce the decrease of the Raman intensity. Although S_8 ring structure is maintained in the liquid phase at temperatures below 432 K, transparency of the sample is increasing in liquid phase, and intensity of Raman scattering is decreasing. Therefore, the transition to liquid phase is expected to induce the decrease in Raman intensity regardless the bond breaking occurs or not. This is easily confirmed by the experiment. A powder sulfur sample was heated up to melt at the ambient pressure and a Raman spectrum of the melted sample was measured. The very weak Raman spectrum was observed as expected, and it was not recovered after the re-solidification by cooling.

When the shock front moves through a molecular solid, the shock produces a temperature increase from an initial temperature T_0 to a temperature T. By assuming that the bulk Grüneisen parameter Γ is independent of T, and $G = \Gamma/V = \Gamma_0/V_0$, T is given by as follows [21)].

$$T = T_0 e^{\Gamma(V_0-V)/V_0} + \int_{V_0}^{V} \frac{f(V)\exp(GV)}{C_V} dV = T_0 e^{\Gamma U_p/U_s} + \Delta T_{irr}$$

$$f(V) = 1/2[(V_0-V)(dP/dV)+P] \tag{3}$$

This equation (3) indicates that the shock temperature jump depends on the bulk Grüneisen parameter Γ, volume compressibility, and irreversible energy transfer. The first term on the right hand side is the temperature increase due to a reversible adiabatic compression, and the second term is the additional temperature increase due to the irreversible compression of the shock. V_0 is the initial volume and V is the volume at pressure P. The bulk Grüneisen parameter Γ can be estimated by a simple method based on the Hugoniot data developed by Nagayama [22), 23)]. A estimated value of Γ=2.75 is in good agreement with the averaged mode Grüneisen coefficient of phonons ($\bar{\Gamma}_{phonon}$ = 2.77) [18)]. To simplify the calculations in what follows, we will ignore the irreversible part of the temperature increase (i.e., ΔT_{irr}=0). This results in a systematic underestimation of the temperature, but it has been shown [24)] that the error due to this assumption is very small up to about 4 GPa. Figure 6 shows the time profile of the temperature derived from values of measured U_p given in Fig. 5. It is assumed that the VISAR probed the back surface of the sample, and the total delay time of 63 ns caused by the VISAR (33 ns), delay in Al foil (8 ns), and delay in the sample (22 ns) is subtracted from the original time scale. As shown in Fig. 6, the temperature increase by the shock compression is small. The maximum temperature is about 350 K, and this temperture is lower than the melting temperature at ambient pressure.

The temperature T can also be derived from the ratio of the anti-Stokes and Stokes intensities [25)]:

Fig. 6   Time profiles of vibrational (dots) and bulk (line) temperature after the shock exitation.

$$\frac{I_{as,\omega_V}}{I_{s,\omega_V}} = \left(\frac{\omega_L+\omega_V}{\omega_L-\omega_V}\right)^4 \exp\left(\frac{-\hbar\omega_V}{k_BT}\right), \tag{4}$$

where $I_{as, \omega v}$ and $I_{s, \omega v}$ are the anti-Stokes and Stokes intensities, respectively, collected over the same scattering solid angle and volume for a particular vibrational mode of the material with energy of $\hbar\omega_V$, ω_L is the laser excitation frequency, k_B is the Boltzman constant. The temperature derived from the equation (4) corresponds to the "vibrational temperature", and can be different form the "bulk temperature" given by the equation (3). In this calculation of vibrational temperature, the correction of the wavelength dependence of the detection system (mainly due to the holographic notch filter) is required. The correction factor for the particular Raman line is easily obtained by measuring the ratio of the anti-Stokes and Stokes intensities at known temperature (i.e., at room temperature). The vibrational temperatures estimated from the measured Raman line at 218 cm^{-1} are shown in Fig. 6. The raise of the vibrational temperature is faster than the bulk temperature, and the vibrational temperature is higher than the bulk temperature. The vibrational temperature goes up to 500 K, which is high enough for the transition from solid to liquid. Such non-equilibrium between the vibrational mode and the other overall degree of freedom is possible if the vibrational excitation due to the shock compression is much faster than the excitation of other modes.

Present experimental results indicated that the vibrational mode is excited very fast (within 50 ns) and this vibrational excitation induces melting of the sulfur. However, the origin of the time delay in "bulk" temperature is still not clear, and further work is required to conclude the mechanism for the nano-shock compression. Such study is in progress.

References
1) B. Meyer, Chem. Rev., 76, 36 (1976).
2) S.T. Rettig and J. Trotter, Acta Cryst. C, 43, 2260 (1987).
3) B. Eckert, R. Schumacher, H. Jodl and P. Foggi, High Pres. Res., 17, 113 (2000).
4) A. Yoshioka and K. Nagata, J. Phys. Chem. Solids, 56, 581 (1995).
5) A.K. Abass and N.H. Ahmad, J. Phys. Chem. Solids, 47, 143 (1986).
6) A.K. Abass, A.K. Hasen and R.H. Misho, J. Appl. Phys., 58, 1640 (1985).
7) M.J. Peanasky, C.W. Jurgensen and H.G. Drickamer, J. Chem. Phys., 81, 6407 (1984).
8) H. Luo and A.L. Ruoff, "High-Pressure Science and Technology", p. 1527 (1993), AIP Press, New York
9) R.O. Jones and P. Ballone, J. Chem. Phys. 118, 9257 (2003).
10) A.V. Tobolsky and A. Eisenberg, J. Am. Chem. Soc., 81, 780 (1959).
11) L. Wang, Y. Zhao, R. Lu, Y. Meng, Y. Fan, H. Luo, Q. Cui, "High-Pressure Research in Mineral Physics", p. 299 (1987), Terra Scientific Publishing, Tokyo.
12) Y.B. Zel'dovich and Y.P. Raizer, "Physics of Shock Waves and High-Temperature Hydrodynamic Phenomena", (1966), Academic press, New York,.
13) J.R. Asay and M. Shahinpoor, "High-Pressure Shock Compression of Solids", (1993), Spring-Verlag, New York.
14) D.D. Dlott, J. Phys. IV, 5(C4), 337 (1995).
15) S.P. Marsh, "LASL Shock Hugoniot Data", (1980), University of California Press, Berkeley, CA.
16) M.F. Gogulya and M.A. Brazhnikov, Zhurnal Tekhnicheskoi Fiziki, 62, 197 (1992).
17) A. Anderson, W. Smith, J.F. Wheeldon, Chem. Phys. Lett., 263, 133 (1996).
18) R. Zallen, Phys. Rev.B, 9, 4485 (1974).
19) C. Pastorino and Z. Gamba, J. Chem. Phys., 112, 282 (2000).
20) P. Ballone and R.O. Jones, J. Chem. Phys., 119, 8704 (2003).
21) V.K. Jindal, and D.D. Dlott, J. Appl. Phys., 83, 5203 (1998).
22) K. Nagayama and Y. Mori, J. Phys. Soc. Jpn., 63, 4070 (1994).
23) K. Nagayama, J. Phys. Chem. Solids, 58, 271 (1997).
24) A. Tokumakoff, M.D. Fayer, D.D. dlott, J. Phys. Chem., 97, 1901 (1993).
25) H. Poulet and J.P. Mathieu, "Vibration Spectra and Symmetry of Crystals", (1976), Gordon and Breach, New York.

レーザ誘起ナノ衝撃波圧縮によるイオウの相転移

叶　樹集，出雲充生，酒井雅貴，越　光男†

　衝撃波が印加されたイオウ結晶の時間分解ラマンスペクトルを観測した。衝撃波はパルス YAG レーザ光をアルミ薄膜に集光してレーザアブレーションを起こさせることにより発生させた。VISAR（レーザ干渉計）により粒子速度を測定し，ランキンーウゴニオの関係式から発生圧力を推定した。試作した装置により，最高 0.7 GPa の圧力パルスが発生できることを確認した。ラマンスペクトルの強度が衝撃波到達後 50 ns 以内に高速に減衰し，衝撃波が追加した後でも強度は回復しないことが見出された。このようなラマンスペクトルの衝撃波による減衰は，衝撃波背後でイオウ結晶が融解しているかまたはアモルファス相への相転移が起こっていることを示している。また，218 cm^{-1} のラマンラインのストークス線と反ストークス線の強度比から評価した振動温度は，ウゴニオ式から予測される衝撃波背後のバルク温度よりも高いことが見出された。

東京大学大学院工学系研究科　化学システム工学専攻　〒 113-8656　東京都文京区本郷 7-3-1
†Corresponding address: koshi@chemsys.t.u-tokyo.ac.jp